Positioning Performance Evaluation of Regional Ionospheric Corrections with Single Frequency GPS Receivers

W Liu, H Zhang, C Wang, Y Feng
Queensland University of Technology, Australia
X Hu
Wuhan University, China

ABSTRACT

Single-frequency (SF) GPS receivers have the potential to become an accurate alternative to high-end dual frequency receivers for many applications such as GIS data collections, vehicle positioning for lane-level safety applications and entertainment. For a single frequency receiver to achieve positioning precision of decimetre level, ionosphere delay is the main bottleneck among all error sources. The IGS-released Global Ionospheric Map (GIM) provides for ionosphere corrections. However, the GIM corrections neither are available for real time applications, nor have the accuracy required to enable single frequency decimetre positioing.

With around 200 reference stations, Australian Regional Ionospheric Corrections (AusRIC) are generated with high temporal and spatial resolution of both the slant and vertical total electron contents (TEC). This paper describes the station-based PPP ionosphere estimation method, which preserve the integer nature for carrier phase ambiguity resolutions. In order to achieve decimetre or higher precision, error sources including DCB, solid earth tide, phase centre offset and windup are taken into consideration, in addition to adoption of precise orbits and clocks.

With the AusRIC generated for the 1st of January 2014, the evaluation is performed with both SF-SPP and SF-PPP modes, based on the modifications to the RTKLib software platform. The SPP solutions from 25 selected reference receivers have shown the decimetre RMS accuracy better than 19 cm for the East/North directions and 55 cm for the Up-component. With the same data sets and receivers, the SF-PPP mode yields the RMS accuracy of better than 10 cm and 25 cm for the horizontal and vertical component respectively.

KEYWORDS: Regional ionospheric corrections, single frequency PPP, single frequency SPP, decimetre positioning

1. INTRODUCTION

GNSS applications may be grouped into several categories according to their requirements on the positioning performance characteristics, such as mass-market, high precision professional, safety-of-life, and scientific categories. To meet different requirements, there have been several types of services up-running available for different categories of users. For instance, GPS Standard Positioning Service (SPS) can directly support mass-market users. Satellite-Based Augmentation System (SBAS) are designed to meet safety-of-life aviation requirements. High-precision professional users are supported by the single-based or network-based Real Time Kinematic (RTK) positioning services. For supporting these applications, International GNSS Service (IGS) has been providing both the real-time and post-processing satellite products and services such as satellite ephemerides, satellite clock and atmospheric corrections.

While the needs of mass-market and high precision applications have been supported with SPS and dual-frequency RTK techniques, there is an increasing need of single-frequency decimetre positioning services for emerging applications, such as Intelligent Transport System (ITS), Unmanned Airborne Vehicle (UAV) and many others. In the instance of ITS, safety applications and lane-level traffic management, vehicles must reliably determine which lanes it is travelling and where in the lane of each surrounding vehicle. The accuracy requirement for this capability is decimetre RMS accuracy in general (Ansari, Wang, Wang, & Feng, 2013; Green et al., 2013). Additionally, GIS data collections with hand-hold units require decimetre positioning accuracy.

There are a number of factors limiting the decimetre positioning capabilities with single-frequency receivers, such as the effects of high receiver noise levels and multipath and the unmodelled or residual tropospheric delay. However, the ionosphere delay is the factor that contributes the most (Kaplan & Hegarty, 2005). Various methods have been developed to mitigate the ionosphere delay for SF receivers. With the Klobuchar model, it is only able to correct 50% of the delay (Klobuchar, 1987) and achieve 4m or 3m precision (Yuan et al., 2008) with the GPS navigation data. The Global Ionosphere Map (GIM) provided by IGS is a 2.5°×5° grid map with 2-hour temporal resolution, generated from a global-scale reference network equipped with dual-frequency receivers. The Line-Of-Sight (LOS) TEC is derived from geometry-free linear combination with phase-smoothed code from the network and then mapped to the vertical direction, refers to as vertical TEC (vTEC) (Feltens, Dow, Martín-Mur, Martínez, & Bernedo, 1998; Hernández-Pajares, Juan, & Sanz, 1999; Mannucci et al., 1998; Schaer, Beutler, & Rothacher, 1998). VTEC is then converted to a grid map employing Spherical Harmonic (SH) expansions with a full set of SH coefficients. It is based on a thin spherical shell at the height of 350km – 400km typically. However, the temporal and spatial characteristics of ionosphere cannot be described accurately in large scale through functional model, its accuracy is in the range of 2~8 TECU (http://igsws.unavco.org/components/prods.html). Researchers have also been investigating Regional Ionosphere Map (RIM) with higher density regional-scale network that is supposed to offer better positioning accuracy than what GIM can support. Results have validated that RIM reaches sub-meter precision with SBAS and SF-Precise Point Positioning (PPP) in several areas (Crespi, Mazzoni, & Brunini, 2012; Zhang et al., 2013). Another approach is to use the slant ionosphere corrections from several surrounding stations in the user positioning processing (Shi, Gu, Lou, & Ge, 2012). This approach has the potential to be used for real-time applications, and the user algorithms can detect and exclude the ionosphere corrections with bad quality or outliers, as demonstrated by Feng, Gu, Shi, and Rizos (2013). Gu, Shi,

Lou, and Liu (2015) has elaborated how the corrections are generated and validated its support for PPP. In this work, this approach is refers to as the Station-based Ionosphere Map (SIM) approach.

Table 1 summarises various services against positioning accuracy requirements and how the ionosphere delays are handled in each approach. It is suggested that the decimetre accuracy can be achieved by SF-single-point-positioning (SPP) amd SF-PPP algorithms if a RIM or SIM model is accurately established. In this work, with Australian Regional Ionosphere Corrections (AusRIC) generated for the January 1 2014, the evaluation is performed on both SF-SPP and SF-PPP modes, based on the modification to the RTKLib software platform. The paper is organised as follows. Section 2 outlines how the SIM and AusRIC are generated based on the reference-station computing approach proposed by Feng et al. (2013). Section 3 examines effects of various error sources that affect decimetre or higher precision, including precise orbits and clocks, DCB, solid earth tide, phase centre offset and windup. Section 4 presents experiments results to demonstrate how ionosphere delay corrections from 200 stations in Australia can support single frequency SPP and PPP for decimetre solutions.

Table 1 Current GNSS application categories and there corresponding solution and ionosphere correction strategies.

Application requirement on precision	Solution	Ionosphere correction
Meter	SPS, PPS	Klobuchar, Global Ionosphere Map (GIM)
Sub-meter	SBAS: WAAS, EGNOS	GIM, Regional Ionosphere Map (RIM)
Decimetre	SPP, SF-PPP	RIM, Station-based Ionosphere Map (SIM)
Centimetre	SF/DF-RTK, DF-PPP	Network RTK, Ionosphere-free (IF)

2. GNSS SIGNAL ERROR SOURCES AND CORRECTIONS

GPS pseudorange and carrier phase observables for each satellite-receiver pair can be expressed as the following observation equation in range units:

$$P_i = \rho - c \cdot t^s + c \cdot t^r + T + I_i - b_i^s + b_i^r + e_{P_i} \tag{1}$$

$$L_i = \rho - c \cdot t^s + c \cdot t^r + T + \Delta\emptyset_{windup} - I_i - \lambda_i \cdot k_i + e_{L_i} \tag{2}$$

where the subscript i refers to frequency f_i, ρ denotes the geometry distance from satellite to receiver, c is the speed of light, t^s and t^r refer to satellite and receiver clock errors, T and I are ionosphere and troposphere delays, b^s and b^r represents satellite and receiver instrumental group delays, λ is carrier wave length, k includes the carrier phase ambiguity and the satellite and receiver instrumental phase delays, windup is the phase windup error, e represents multipath, noise, and antenna phase centre offset. Among all error sources, ionosphere-delay is the one that contributes the most.

2.1 Ionosphere delay corrections

During AusRIC generation, the slant TEC values along signal paths for each stations are computed from raw data to form the SIM product. This is then converted to form Regional Ionosphere Map (RIM) with Inverse Distance Weighting (IDW) method or the SH function as what GIM uses. Even though the overall concept is similar to the GIM provided by IGS, there is a funcdemntal differnece in the extraction of the slant TEC values from raw data.

Using the reference-station computing approach proposed by Feng et al. (2013), the raw data streams from each GNSS reference station are processed individually, to generate station-based solutions. The processing strategy is similar to PPP technique, where satellite orbits, clocks and satellite-specific instrumental delay bias provided by IGS products, and the dry component of the zenith tropospheric delay ZTD_d predicted by standard metrological model, except that the position vector of satellite and station are held fixed. Accordingly, the observable residuals between observed values and computed values are derived as follows.

$$dP_i \equiv P_i - (\rho - c \cdot t^s + tropm_d ZTD_d - b_i^s)$$

$$= c \cdot t^r + tropm_w ZTD_w + \frac{f_1^2}{f_i^2} I_i + b_i^r + e_{P_i} \qquad (3)$$

$$dL_i \equiv L_i - (\rho - c \cdot t^s + \Delta\emptyset_{windup} + tropm_d ZTD_d)$$

$$= c \cdot t^r + tropm_w ZTD_w - \frac{f_1^2}{f_i^2} I_i - \lambda_i \cdot k_i + e_{L_i} \qquad (4)$$

The station-based approach aims to determine all the biases in the right-hand side of equations (3) and (4), including receiver-specific parameters (clock, wet component of ZTD, instrumental code delay) and satellite-specific parameters (observable residuals, float ambiguity solution, tropospheric mapping function, ionospheric mapping function, vTEC and its standard deviation). Being different from geometry-free linear combination, the method to solve the ionospheric delay uses the geometry-based model (Gu, 2013). The raw data on each frequency is used to aid estimation of ionospheric delays. The ionospheric zenith delay is represented by a set of parameters of latitude and longitude, which are then estimated alongside other parameters such as phase ambiguities, ZTD, and receiver position and clocks. To minimize the convergence time, the GIM provided by Centre of Orbit Determination in Europe (CODE) can be treated as a priori information of ionospheric delay. In addition, to accurately describe the station-based temporal and spatial ionospheric feature, a stochastic process is introduced (Bock, Jäggi, Dach, Schaer, & Beutler, 2009). As a result, the ionospheric delay can be expressed as:

$$I_i = ionom \cdot (a_0 + a_1 dL + a_2 dL^2 + a_3 dB + a_4 dB^2 + r(t)) \qquad (5)$$

where $ionom$ is the mapping function, a_0 denotes the average delay over the station, a_1, a_2, a_3 and a_4 are unknown coefficients of polynomial model, dL and dB are the latitude and longitude differences between IPP and station.

While all the biases in the equations (3) and (4) are determined, plus elevation and azimuth angles as part of outputs, they can be accessed by nearby users through a unified format-site solution exchange (SITEX) format as proposed by Feng et al (2013), making the station-based and user-based algorithms consistent with each other. Especially, since the ionospheric delays vary rapidly, quality control is required for reliability. Therefore, their standard deviations are provided as well. As a result, SIM is generated from the ionospheric corrections in SITEX files, and then RIM is established for IPP layer using the models mentioned at the beginning of this section. In addition, this method supports ambiguity-fixed PPP especially. Through single-differencing between satellites, the receiver clock bias and reference station ambiguity are cancelled, whereby the integer nature for carrier phase ambiguity resolution is preserved.

From users' perspective, with RIM, one first finds the nearest four points on the ionosphere layer, and interpolates his own ionosphere delay according to latitude, longitude, and elevation, as illustrated by Figure. We can repeat the same step for another nearest epoch, and do linear interpolation by time.
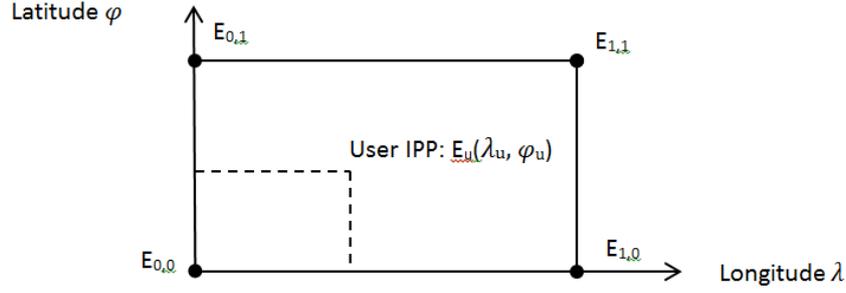
Figure 1 How user deals with RIM data.

With SIM, users may access a nearby station and directly apply the same correction for that station. But it is only applicable for short baseline and high elevation angle, since ionosphere delay is location and elevation-dependent. The complete SIM method is to select several surrounding stations in the range of a certain baseline length threshold and to interpolate the correction of each LOS signal for user receiver ($sTEC_{user}$) with slant TEC values of surrounding stations ($sTEC^{ref}$) according to their relative geographical locations (D^{ref}_{user}): Figure 2 demonstrated the concept.

$$sTEC_{user} = \frac{\sum_{ref=1}^{n} \frac{sTEC^{ref}}{D^{ref}_{user}}}{\sum_{ref=1}^{n} \frac{1}{D^{ref}_{user}}} \, for \quad (D < threshold) \tag{6}$$
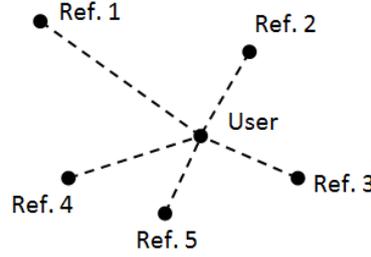

Figure 2 How user deals with SIM data.

When employing SIM, the obvious advantage is that users don't need to receive too much data. Only the data from surrounding base stations is necessary. Therefore, SIM has the potential for real-time applications. Another advantage is that by weighting, it is possible to test and exclude some stations whose data is of bad quality for further precision improvement.

2.2 Corrections for other error sources

It is very difficult to synchronize the signals with clocks in both satellite and receiver, because of Differential Code Biases (DCB). It is hardware instrumental biases, the time delay between observed and referenced pseudorange $\Delta t^s_{obs-ref}$. It introduces systematic errors when estimating ionosphere delays (Sardon, Rius, & Zarraoa, 1994),

$$I^s_{1,r} = \frac{P^s_{1,r} - P^s_{2,r}}{1-\gamma} - \left(\frac{DCB^s + DCB_r}{1-\gamma}\right) \cdot c + \frac{m^s_{2,r} - m^s_{1,r}}{1-\gamma} + \frac{v^s_{2,r} - v^s_{1,r}}{1-\delta} \tag{7}$$

where *m* and *v* stand for multipath and noise respectively. The time of group delay (T_{GD}) is the difference of the time from generation to transmission for L1 and L2 signals (L1-L2

correction). It can be obtained from navigation message, and its clock is referenced to P1. For P2 measurement, Δt_{P2-P1}^s is directly related to T_{GD} by frequency (Rho & Langley, 2007).

$$\Delta t_{P2-P1}^s = (\gamma - 1)T_{GD}, \; \gamma = \frac{{f_1}^2}{{f_2}^2} \tag{9}$$

Apart from DCB, the inaccurate satellite clock measurement could introduce several decimetres' error, making combining pseudorange data with IGS precise clock products necessary. These products are referenced to C1. Therefore, T_{GD} and $\Delta t_{obs-ref}$ should be stamped on satellite clock errors, while ref depends on whether the precise clock correction is applied. For P1 measurement, Δt_{P1-P1}^s equals to zero.

$$correction \; of \; t^s = \begin{cases} t^s - T_{GD} - \Delta t_{P1-P1}^s & without \; precise \; clock \\ t^s - T_{GD} - \Delta t_{P1-C1}^s & with \; precise \; clock \end{cases} \tag{8}$$

However, T_{GD} and DCB do not need to be taken into account for all kinds of users. Receivers working in relative positioning mode can eliminate the impact of DCB by the double differencing technique. Dual-frequency receivers using ionosphere-free linear combination, need DCB calibration but not T_{GD}. Only single-frequency receivers working in absolute positioning mode require the external DCB calibration. It has been provided by CODE's monthly generated P1-CI table.

Furthermore, the measurements are made to the antenna phase centre, so are the orbits broadcasted in navigation messages. However, the IGS-released precise satellite coordinates and clock products refer to the satellite centre of mass (Kouba & Héroux, 2001). Therefore, correction on phase centre offset is compulsory if IGS precise ephemeris and clock are applied. On the other hand, Because the stations are on the ground, when decimetre or higher precision is required, the weakly fluctuated vertical and horizontal site displacements that depend on station latitude and tidal frequency (Wahr, 1981) need to be taken into account. Omitting the solid earth tides effect, vertical positioning precision could be degraded to 0.4 m at maximum. In addition, phase wind-up must be taken into consideration as well.

3. EVALUATION STRATEGY AND RESULTS

To validate the above theoretical analysis, several experiments are conducted based on the modification to the RTKLib software platform. First, the qualities of station-based and regional Australian ionospheric corrections are evaluated. Then, the analysis focuses mainly on SIM performance on single frequency receivers. The comparison of using three ionospheric delay correction strategies is given in the final part. Data processing configuration is demonstrated in Table 2, elaborating how parameters are used in different modes. The CODE ionospheric grid map is employed as GIM, while RIM and SIM are derived from SITEX files.

Data is collected on the January 1 2014 from about 200 stations within Australia for RIM generation, as are presented with red dots in Figure 3, 25 of which are treated as user receivers that are marked by blue dots. CODE-released GIM is employed for comparison. It is generated from 400 global stations, but only 20 of which belong to Australia. Green dots illustrate their locations. Figure 4 demonstrates the spatial resolution of these two ionospheric grid maps covering -55°~0° in latitude and 105°~165° in longitude. Evidently, AusRIC at

bottom row provides more ionosphere characteristics in detail because of higher station density and appropriate algorithm. To evaluate the RIM and GIM quality, the LOS TEC values in station-based map is regarded as true value. The difference of global or regional vTEC and the "real" vTEC are presented with the increasing of elevation angle in Figure 5. Each calculation is conducted at the same IPP latitude and longitude. Specifically, station-based map is updated every epoch (30 seconds) and regional map is updated every five minutes. Since vertical ionosphere delay is fairly stable within 10 minutes (Blanch, 2003), and five-minute-resolution is short enough to provide with high accuracy in this experiment. The spatial resolution for both global and regional map is $2° \times 2.5°$. There is a descending trend in the difference with the elevation growing, because lower elevation introduces in a greater mapping error when converting the ionosphere delay from slant to vertical, and vice versa. The 1σ RMS values are 3.6 TECU for GIM, and 0.2 TECU for RIM.

Table 2 Data processing strategies

| Configuration	PPP	SPP
Ionosphere delay	GIM, RIM, SIM	GIM, RIM, SIM
Troposphere delay	Estimated	Saastamoinen model
Ephemeris & clock	IGS final product	IGS final product
PCO/PCV	Corrected	Corrected
Solid earth tides	Corrected	Corrected
Phase windup	Corrected	Not corrected
Elevation angle cutoff	10°	10°
Sample rate	30s	30s
Coordinate	Estimated	Estimated
Clock	Estimated	Estimated
DCB	IGS product	IGS product
Ambiguity	Continuous	
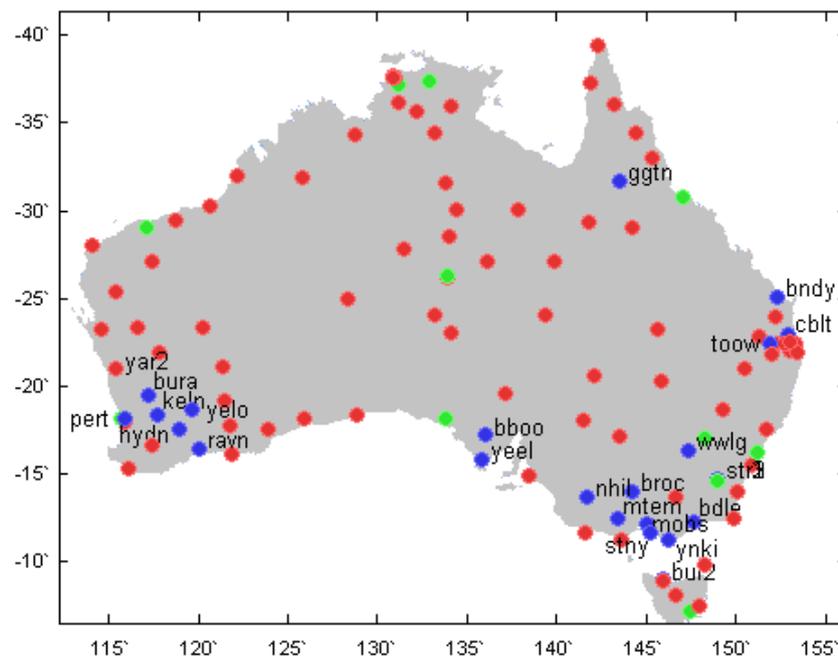
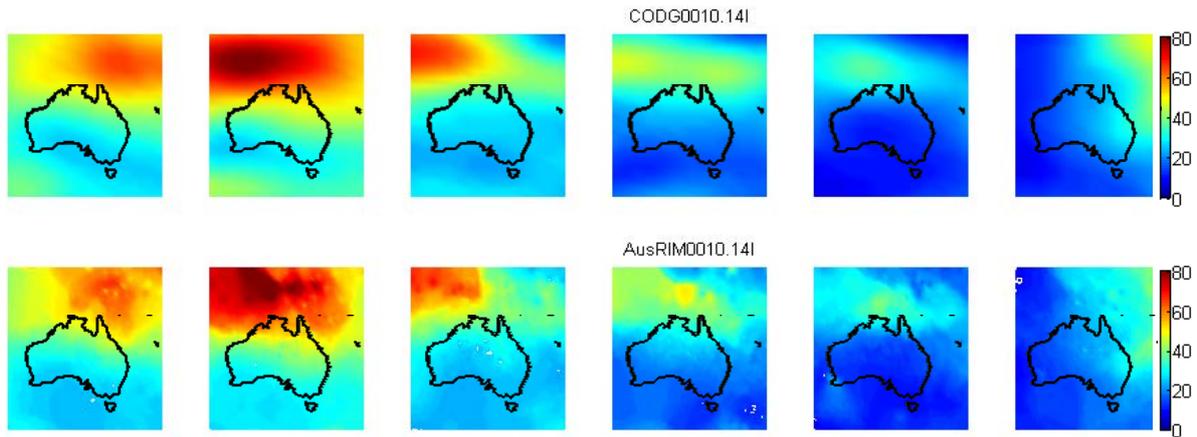**Figure 3** Australian stations employed for GIM (green) and for AusRIC generation (red).

Figure 4 Australian vTEC maps provided by GIM (top row) and RIM (bottom row) at epochs 0200UT, 0600UT, 1000UT, 1400UT, 1800UT, 2200UT from left to right columns.
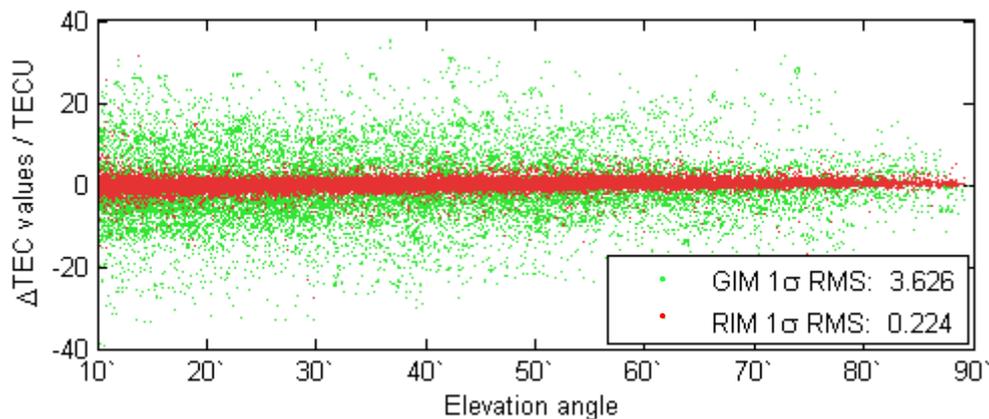

Figure 5 Quality analysis of GIM and RIM, represented by the differences between grid map vTEC and station-based vTEC.

Applying the reference station-based processing approach introduced in section 2.1, positioning results using SIM corrections with different baseline lengths are calculated at the 25 user receivers as plotted in Figure 3 in blue dots. The baseline length threshold as radius is selected from 150km to 300km, with a step of 50km. The longer radius leads to the more surrounding stations to be included. SPP and PPP results at three directions are demonstrated in Figure 6 and 7 separately, through which it cannot be concluded that the positioning precision is positively or negatively correlated with the increase of surrounding station numbers. Take station BURA as an example, whose surrounding stations are symmetrically distributed according to figure 3, the more stations included, the better the precision is obtained on both modes and in all directions. However, for BNDY all the surrounding stations are on its south side, the more stations utilized, the more southern they are to the user, leading to the precision degradation. Similarly, all the baseline distances for GGTN within 300km are around 280km, rendering the distance-dependent ionosphere correction inaccurate. In this case, the station geometrical distribution needs to be quite symmetrical and compact. Under most situations, radius of 300km is appropriate in order to cover five surrounding stations on average. User in locations like BNDY should just take the correction from the nearest station instead of interpolation.

The quality of ground-interpolated SIM method is further analysed through combining the biases for all satellites above the cut-off angle of 10°. Figure 8 upper panel gives an example
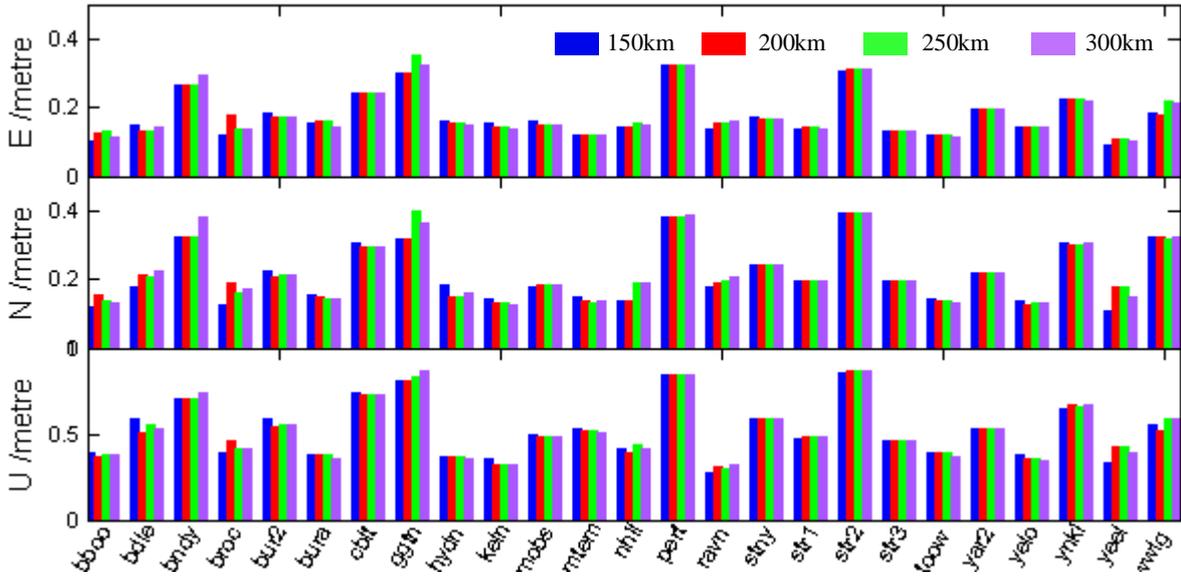
Figure 6 SPP positioning precision with SIM with different radius lengths.
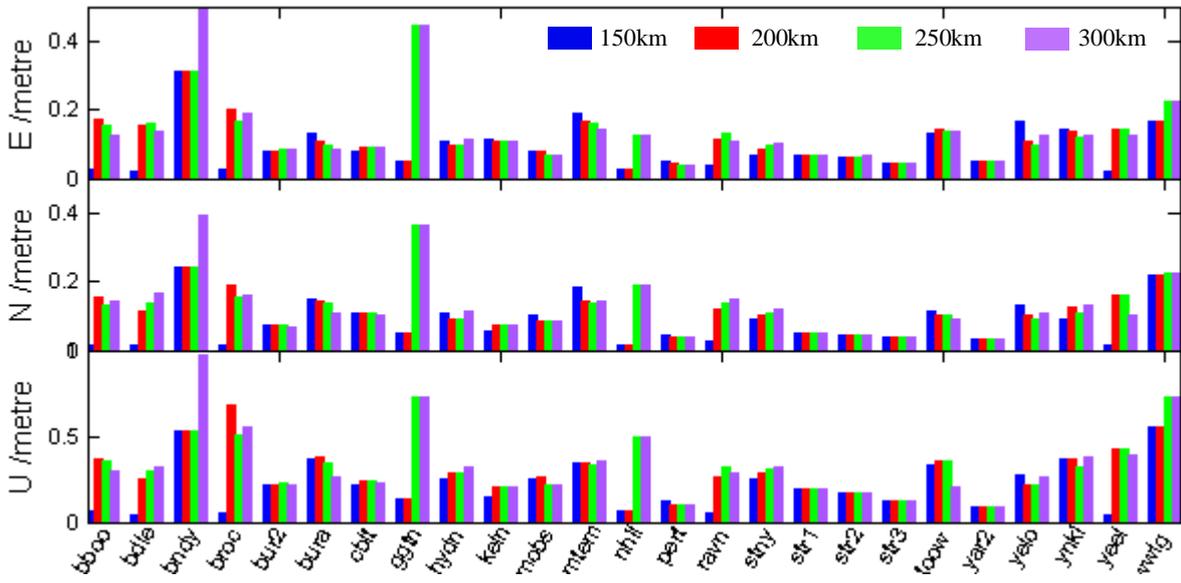

Figure 7 PPP positioning precision with SIM with different radius lengths.

at station STR2. There are several outliers: biases of PRN 24 and PRN 4 (the inserted part) reach -4 and -6 TECU, which will cause large errors of 0.64m and 0.96m along their L1 signal paths, respectively. These evident deviations can be easily eliminated. Then the RMS value of biases are calculated and plotted in the lower panel in Figure 8 epoch-to-epoch. And then the RMS through the whole day is calculated, and equals to 0.226 TECU, which corresponds to a few centimetres, indicating that as a whole the error of interpolating with surrounding stations is acceptable for decimetre level applications. Figure 9 shows the all-day RMS for the 25 user receivers in total, 68% of which are under 0.5 TECU.

With the above analysed station-interpolated SIM method, five-minute-updated RIM, and CODE-GIM ionospheric corrections, the all-day SPP and SF-PPP positioning results at station TOOW are plotted in Figure 10. Good consistency is evident between SIM and RIM solutions, while the GIM deviations have greater fluctuations, especially in vertical direction.

Except for positioning precision, convergence time as well is a crucial factor of the PPP technique. In the sense of decimetre accuracy, there is no plain convergence time for all three strategies. Figures 11 and 12 show the ENU RMS values of all 25 user receivers on the two modes separately. It is interesting to note that solutions using the RIM sometimes even give a better, epoch-to-epoch accuracy than the SIM approach. More specifically, their 1σ RMS values are summarized in Table 3. The SF-SPP solutions from 25 selected reference receivers prove the decimetre RMS values using AusRIC, which is reduced from 32 cm to 19 cm for East/North component and from 72 cm to 55 cm for Up-component, comparing to GIM method. With the same data sets and receivers, the SF-PPP mode reduces the RMS values from 25 and 55 cm to 13 cm and 34 cm in the two components. With SIM, the precision of SF-PPP solution is better improved to RMS value of 10 and 25 cm in two directions.
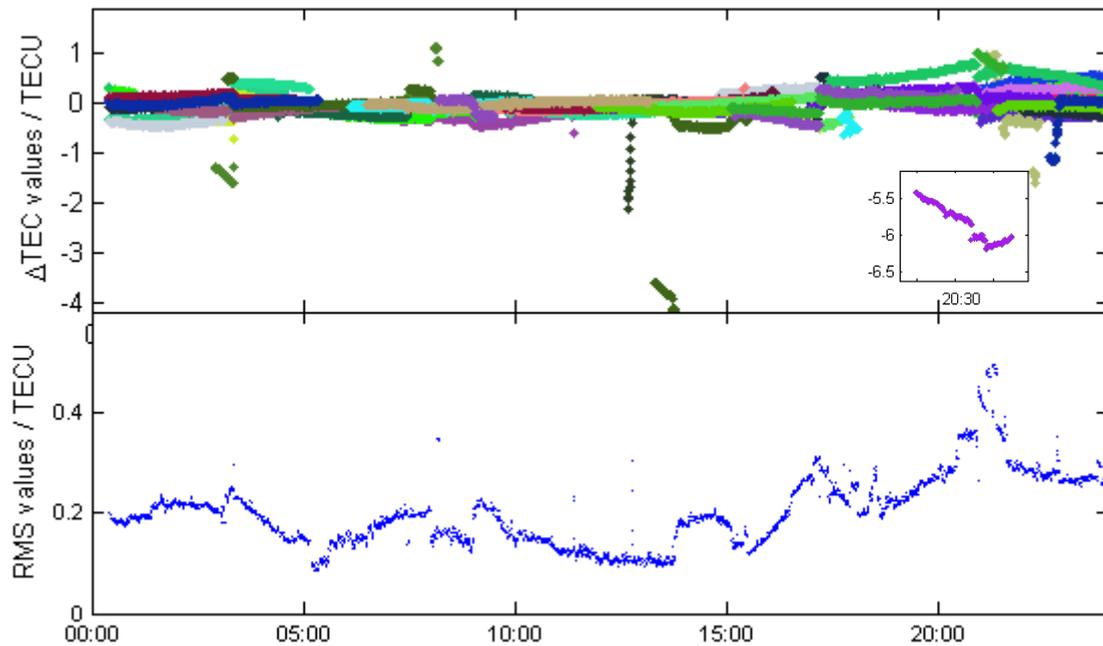

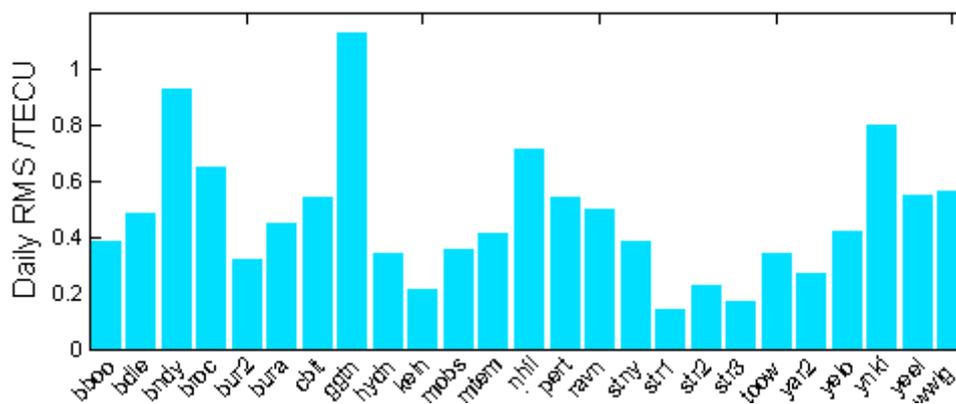**Figure 8** Biases for all satellites through the whole day and the RMS values of biases.

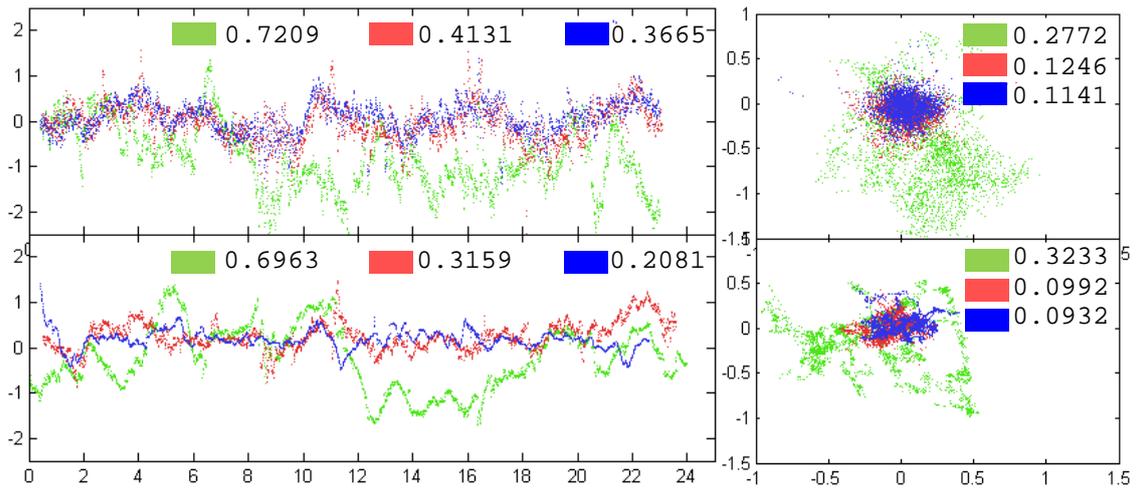**Figure 9** RMS values for 25 user receivers.

Figure 10 Positioning deviations at station TOOW on both SPP (top row) and PPP (bottom row) modes, with three different ionosphere corrections (GIM in green, RIM in red, and SIM in blue). Results are represented in vertical (left column) and horizontal (right column) directions.
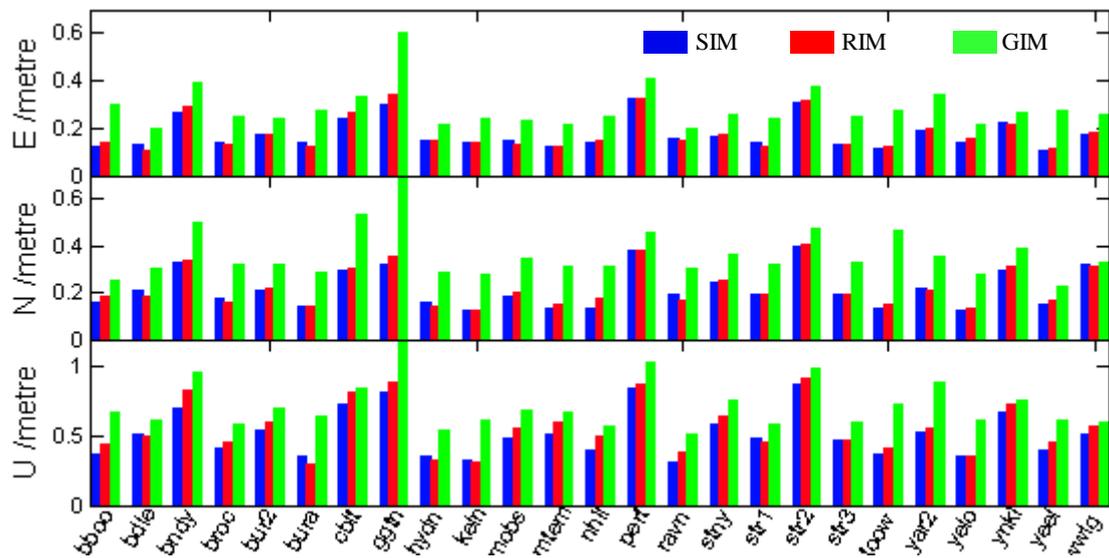

Figure 11 Positioning precision at East, North, Up directions for 25 stations on SPP processing mode with GIM, RIM, and SIM corrections respectively.
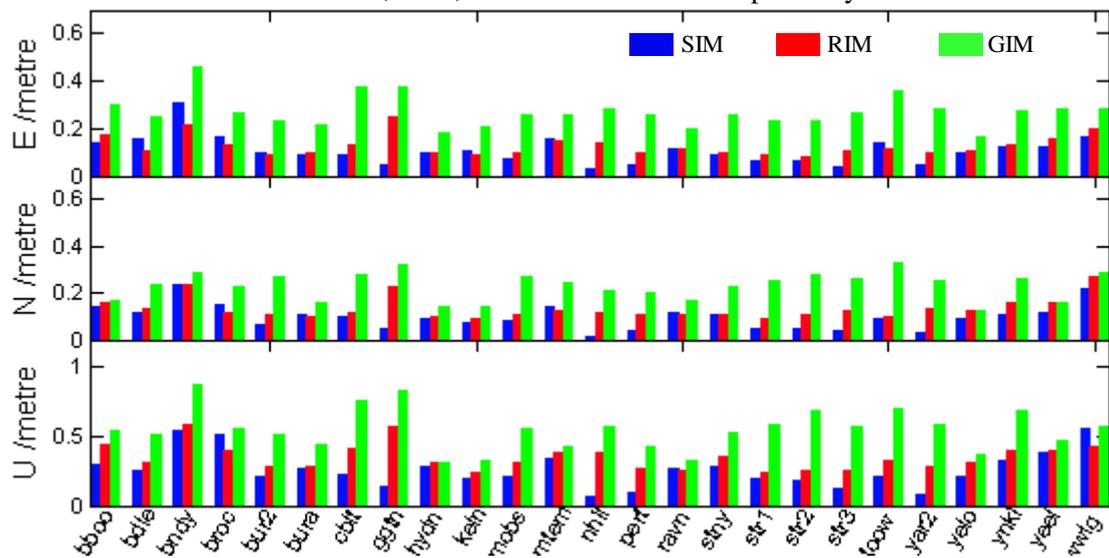

Figure 12 Positioning precision at East, North, Up directions for 25 stations on PPP processing mode with GIM, RIM, and SIM corrections respectively.

Table 3 Total RMS values in meters at three directions computed with three ionospheric correction strategies on SPP and SF-PPP modes.

RMS / m		SPP	SF-PPP
GIM	E	0.284	0.269
	N	0.360	0.227
	U	0.715	0.545
RIM	E	0.178	0.125
	N	0.222	0.131
	U	0.553	0.344
SIM	E	0.175	0.106
	N	0.216	0.096
	U	0.513	0.254

4. CONCLUSIONS

This paper has developed the capability for generating regional ionosphere correction to support single-frequency SPP and PPP in Australia. SIM and RIM are derived with hundreds of stations. Its generation methodology is reviewed in detail from observation equation to SITEX file. The quality of regional map is analysed and its RMS accuracy is proved to range from 0.2 to 1 TECU at user end, depending on the user's locations. Based on modification on RTKLib, this paper especially evaluated the station-based interpolation approach with SIM by calculating the epoch-to-epoch and all-day RMS errors of each signal path, and conclude that quality of interpolating with surrounding stations is acceptable for sub-meter or decimetre level applications. In addition, it is believed that baseline length of 300 km is appropriate in general. As a result, distinct improvement is demonstrated with AusRIC compared with GIM, and decimetre positioning precision is proved. Overall, this work demonstrates the promising potential for the Australia GNSS network to offer decimetre positioning services with single-frequency GNSS receivers, supporting many new emerging applications over Australia. In addition, testings for low-end solutions are on-going at QUT.

REFERENCES

Ansari, K., Wang, C., Wang, L., & Feng, Y. (2013). *Vehicle-to-vehicle real-time relative positioning using 5.9 GHz DSRC media.* Paper presented at the Vehicular Technology Conference (VTC Fall), 2013 IEEE 78th.

Blanch, J. (2003). *Using Kriging to bound satellite ranging errors due to the ionosphere.* Stanford University.

Bock, H., Jäggi, A., Dach, R., Schaer, S., & Beutler, G. (2009). GPS single-frequency orbit determination for low Earth orbiting satellites. *Advances in Space Research, 43*(5), 783-791.

Crespi, M., Mazzoni, A., & Brunini, C. (2012). Assisted Code Point Positioning at Sub-meter Accuracy Level with Ionospheric Corrections Estimated in a Local GNSS Permanent Network *Geodesy for Planet Earth* (pp. 761-768): Springer.

Feltens, J., Dow, J., Martín-Mur, T., Martínez, C. G., & Bernedo, P. (1998). ROUTINE PRODUCTION OF IONOSPHERE TEC MAPS AT ESOC-FIRST RESULTS.

Feng, Y., Gu, S., Shi, C., & Rizos, C. (2013). A reference station-based GNSS computing mode to support unified precise point positioning and real-time kinematic services. *Journal of Geodesy, 87*(10-12), 945-960.

Green, D., Gaffney, J., Bennett, P., Feng, Y., Higgins, M., & Millner, J. (2013). Vehicle positioning for C-ITS in Australia (background document).

Gu, S. (2013). *Research on the Zero-difference Un-combined Data Processing Models for Multi-frequency GNSS and Its Applications.* Wuhan University.

Gu, S., Shi, C., Lou, Y., & Liu, J. (2015). Ionospheric effects in uncalibrated phase delay estimation and

ambiguity-fixed PPP based on raw observable model. *Journal of Geodesy*, 1-11.

Hernández-Pajares, M., Juan, J., & Sanz, J. (1999). New approaches in global ionospheric determination using ground GPS data. *Journal of Atmospheric and Solar-Terrestrial Physics, 61*(16), 1237-1247.

Kaplan, E. D., & Hegarty, C. J. (2005). *Understanding GPS: principles and applications*: Artech house.

Klobuchar, J. A. (1987). Ionospheric time-delay algorithm for single-frequency GPS users. *Aerospace and Electronic Systems, IEEE Transactions on*(3), 325-331.

Kouba, J., & Héroux, P. (2001). Precise point positioning using IGS orbit and clock products. *GPS Solutions, 5*(2), 12-28.

Mannucci, A., Wilson, B., Yuan, D., Ho, C., Lindqwister, U., & Runge, T. (1998). A global mapping technique for GPS‐derived ionospheric total electron content measurements. *Radio science, 33*(3), 565-582.

Rho, H., & Langley, R. B. (2007). Dual-frequency GPS precise point positioning with WADGPS corrections. *NAVIGATION-LOS ANGELES AND WASHINGTON-, 54*(2), 139.

Sardon, E., Rius, A., & Zarraoa, N. (1994). Estimation of the transmitter and receiver differential biases and the ionospheric total electron content from Global Positioning System observations. *Radio science, 29*(3), 577-586.

Schaer, S., Beutler, G., & Rothacher, M. (1998). *Mapping and predicting the ionosphere.* Paper presented at the Proceedings of the 1998 IGS Analysis Center Workshop, Darmstadt, Germany.

Shi, C., Gu, S., Lou, Y., & Ge, M. (2012). An improved approach to model ionospheric delays for single-frequency Precise Point Positioning. *Advances in Space Research, 49*(12), 1698-1708. doi: http://dx.doi.org/10.1016/j.asr.2012.03.016

Wahr, J. M. (1981). The forced nutations of an elliptical, rotating, elastic and oceanless Earth. *Geophysical Journal International, 64*(3), 705-727.

Yuan, Y., Huo, X., Ou, J., Zhang, K., Chai, Y., Wen, D., & Grenfell, R. (2008). Refining the Klobuchar ionospheric coefficients based on GPS observations. *Aerospace and Electronic Systems, IEEE Transactions on, 44*(4), 1498-1510.

Zhang, H., Gao, Z., Ge, M., Niu, X., Huang, L., Tu, R., & Li, X. (2013). On the convergence of ionospheric constrained precise point positioning (IC-PPP) based on undifferential uncombined raw GNSS observations. *Sensors, 13*(11), 15708-15725.